The effect of water vapour on fume formation in a SiMn alloy system

Conference Paper · February 2018

CITATION
1

READS
24

4 authors, including:

Yan Ma
Norwegian University of Science and Technology
5 PUBLICATIONS **6** CITATIONS
SEE PROFILE

Elmira moosavi-khoonsari
Norwegian University of Science and Technology
21 PUBLICATIONS **47** CITATIONS
SEE PROFILE

Gabriella Tranell
Norwegian University of Science and Technology
90 PUBLICATIONS **711** CITATIONS
SEE PROFILE

Infacon XV: International Ferro-Alloys Congress, Edited by R.T. Jones & P. den Hoed,
Southern African Institute of Mining and Metallurgy, Cape Town, 25–28 February 2018

The effect of water vapour on fume formation in a SiMn alloy system

Yan Ma[1], Elmira Moosavi-Khoonsari[1], Ida Kero[2] and Gabriella Tranell[1]
[1]Norwegian University of Science and Technology (NTNU); Alfred Getz vei 2, NO-7491 Trondheim, Norway
[2]SINTEF Materials and Chemistry; Alfred Getz vei 2, NO-7465 Trondheim, Norway[2]

Keywords: liquid SiMn, fume, water, humidity

Abstract – During the tapping, refining and casting processes of manganese ferroalloys, there is a considerable amount of fume generated when the high temperature molten metal vaporizes and oxidizes in the air atmosphere. Fume formation is undesired from a work environment perspective and its spreading outside plant premises may be detrimental to local communities. Experimental studies and industrial observations indicate that the fume generated from the casting of ferromanganese (FeMn) alloy can be significantly reduced by increasing the humidity above the molten metal. However, it is also important to understand the effect of water vapour on the fuming rate of silico-manganese (SiMn) alloys. Laboratory scale experiments were carried out by varying the humidity in an impinging air jet blown onto the surface of a SiMn alloy melt. The fuming rate and fume characteristics (composition, morphology) in the wet air experiments were compared with dry air experiments. The fume composition was also thermodynamically simulated for different gas compositions, using FactSage 7.1.

INTRODUCTION

One of the main environmental challenges facing the ferroalloy industry is fugitive emissions. In a manganese ferroalloy plant, fugitive emissions are generated during material handling and transportation, smelting, refining and casting processes [1]. The fumes include both mechanically generated fume and thermally generated fume. Thermally generated fumes, which are generated during the tapping, refining and casting of alloys, are difficult to capture and hence partly released to the working environment. An installation of fine water sprays along the edge of the roof by the casting beds for FeMn alloys at Eramet Sauda, Norway, has resulted in a significant reduction of the visible fuming emissions[2, 3]. The mechanism by which these sprays of water above a FeMn melt reduces fuming, has been studied in the laboratory[4]. However, there has been no such published study – industrial or laboratory - for the SiMn alloy system. From an industrial perspective, it is important to understand if water sprays would have the same effect on the SiMn system or not. In this work, the effect of varying water vapour pressures on the rate and product of fuming from a standard liquid SiMn alloy was investigated experimentally in laboratory scale, as well as thermodynamically modelled.

BACKGROUND

Thermally generated fumes are formed through the reaction between high temperature liquid metal and oxidative gas species in the atmosphere. In this oxidation process, the main elements in the SiMn alloy (Si and Mn) behave differently. While Mn exhibits high vapour pressure at elevated temperatures, Si forms SiO gas at low oxygen partial pressures. Both gas species oxidise in air and produce complex fumes. The kinetics and

thermodynamics of fume formation from oxidation of liquid SiMn alloy under dry synthetic air at different temperatures has previously been studied by the current authors[5]. Experiments were conducted by heating commercial grade standard SiMn alloy in a closed graphite crucible. A fume/gas extraction system was connected to the crucible lid. During the oxidation process, oxygen will first react with Mn(g) above the melt and form MnO molecular clusters. Some of the MnO clusters may further react with oxygen and form higher oxides. When oxygen diffuses from the bulk gas through the gas boundary layer to the melt surface, SiO(g) molecules are formed by reaction between oxygen and liquid Si. The SiO molecules tend to form SiO clusters which react with and collect the surrounding gas, e.g. O_2 and Mn. The larger clusters, which are composed of a combination of liquid Si and Mn oxide species (molten due to the exothermic oxidation reactions), may or may not crystallize during the solidification process, and exhibit mainly spherically shaped particles as a result[5]. The morphology and composition of SiMn fume largely depend on the melt temperature. In the low melt temperature range (1400°C and 1450°C), the SiO(g) pressure is low and Mn vapour is the main fume-forming gas, resulting in predominantly crystalline manganese oxide in the fume. However, in a medium melt temperature range, between 1500°C to 1600°C, the SiO pressure is higher and most of the MnO formed reacts with SiO molecules/clusters, resulting in complex, amorphous $SiMnO_x$ particles. At high melt temperatures (>1600°C), the Mn evaporation is extensive, resulting in a combination of the complex, amorphous $SiMnO_x$ particles and MnO_x particles[5].

Gates and co-authors[2] initially endeavoured to understand the possible mechanisms of fume suppression by water sprays at Eramet Sauda by modelling. The possible suppression mechanisms evaluated included: high humidity in the casting bed area may reduce the oxygen partial pressure and thus inhibit the oxidation reaction; the change in oxygen partial pressure cause passive oxidation to occur. They concluded that the oxygen reduction mechanism is the most likely mechanism. Gates[4] later studied the oxidation process of High Carbon Ferromanganese (HC-FeMn) alloy in the laboratory by introducing a laminar impinging air jet with different moisture contents blowing onto the melt. It was further illustrated that an increase in water content decreases the relative fume mass flux from the FeMn alloy .

Næss and co-authors[6] conducted similar experiments with pure liquid Si. The study was carried out to better understand the Si fuming rate under various oxidizing conditions. While not an extensive study, two humid air experiments were performed in which synthetic air was bubbled through through a water bath at 25°C before being blown over the melt surface. With the Si alloy, the humidity in the gas (p_{H2O}(g)=0.03atm) brought a small increase in the rate of fume formation rather than a decrease.

EXPRIMENTAL

The wet air experimental set-up is shown in Figure 1. The graphite crucible (Ø150mm, H400mm) was heated to the desired temperature in an Inductotherm 75kW induction furnace - essentially the same as used in our previous studies [5-8], but with the additional humidifier connected with the air supply lance. A standard grade SiMn alloy, composed of 68.03 wt% Mn, 17.58 wt% Si, 11.09 wt% Fe and 2 wt% C as well as minor and trace elements were used for the investigation. The experiments were carried out at different water pressures with the melt temperature at 1450°C or 1600°C. The experimental matrix is shown in Table I. A reference experiment with only dry air at 1600°C was also carried out.

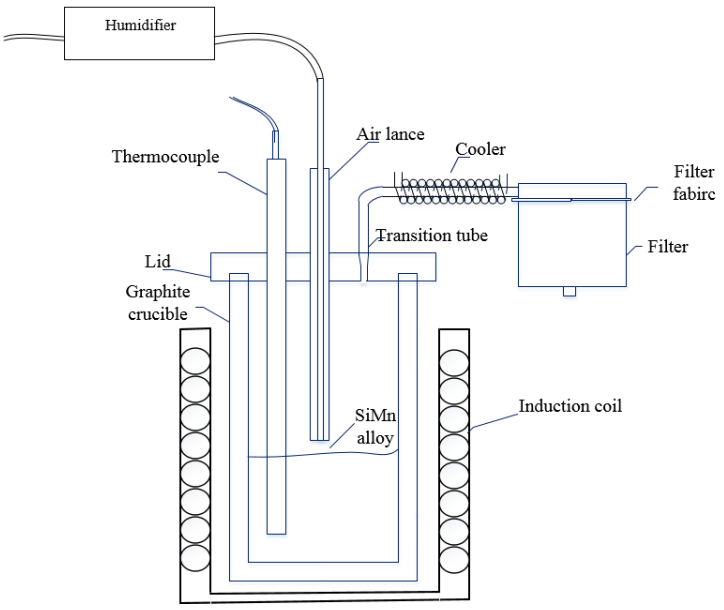

Fig. 1 The experimental set-up

Table I: Experimental matrix

Gas	Melt Temp (°C)	Water pressure/kPa	No of exp.	Holding time/min
Synth. air	1450	7.36	1	25
Synth. air	1450	12.33	1	40
Synth. air	1450	19.92	1	40
Synth. air	1450	25.01	1	40
Synth. air	1600	0	1	30
Synth. air	1600	3.14	3	30, 30 and 40
Synth. air	1600	7.36	3	30, 30 and 40
Synth. air	1600	12.33	4	20, 30, 30 and 40
Synth. air	1600	19.92	3	30, 30 and 40

The Antoine equation was used to calculate the water vapour pressure at a given temperature[9], reported in Table I:

$$\boldsymbol{ln\, P_v\,(Pa) = 23.1963 - \frac{3,816.44}{T\,(K) - 46.13}} \qquad \textbf{(1)}$$

where P_v is the water pressure and T the absolute temperature.

For each experiment, the graphite crucible was filled with 4kg SiMn alloy, and covered by a graphite lid where a fume exhaust system was also connected. During the experiment, dry synthetic air with the gas flow rate 3L/min would initially go through the humidifier to get desired humidity, before blowing above the metal surface. After the experiments, the fume was collected at three sites: the so-called transition tube, the cooler and the filter. The majority of fume was collected from the filter. The transition tube, cooler and filter fabric together with the collected fume were all weighted directly after the experiment, and reweighed again after being dried for at least 20 mins at 110°C. This is done to ensure no water was trapped inside the fume.

There were only visible liquid droplets found at 1450°C when the water pressure was above 12kPa. However, there were no visible liquid droplets found at 1600°C, and almost no mass difference before/after the equipment (containing fume) was dried.

The temperatures in the transition tube, cooler and filter were measured by using an Omega thermometer and K-type thermocouple during the experiment and showed

almost the same temperatures as previously reported [5]. There was about 400°C difference in the transition tube, from about 600°C at the transition tube entry point to around 200°C at the point of connection to the cooler. Inside the cooler, the temperature dropped further to room temperature, and the filter kept constant at almost the same temperature. However, while these temperatures were measured on the surface of the equipments, the inside /off gas temperatures should be relatively higher.

The total amount of fume generated in each experiment is measured and calculated as mass flux J_m,

$$J_m = \frac{m}{At} \tag{2}$$

J_m is the mass flux, m is the total mass of fume generated, A is the surface area of the molten metal (assuming no surface oxide/slag coverage) and t is the holding time of the experiment. The fume collected from the three deposition sites at the 1600°C experiments were characterized by scanning electron microscopy (SEM) together with energy dispersive x-ray spectroscopy (EDS) and x-ray diffraction (XRD).

RESULTS AND DISCUSSION

Mass flux

The mass fluxes obtained from exposing the SiMn alloy to wet and dry air at 1450°C and 1600°C [5, 7] are both shown below in Figure 2. The mass flux is plotted as a function of increasing water pressure. The dry synthetic air experiments are listed with the water pressure of 0 kPa.

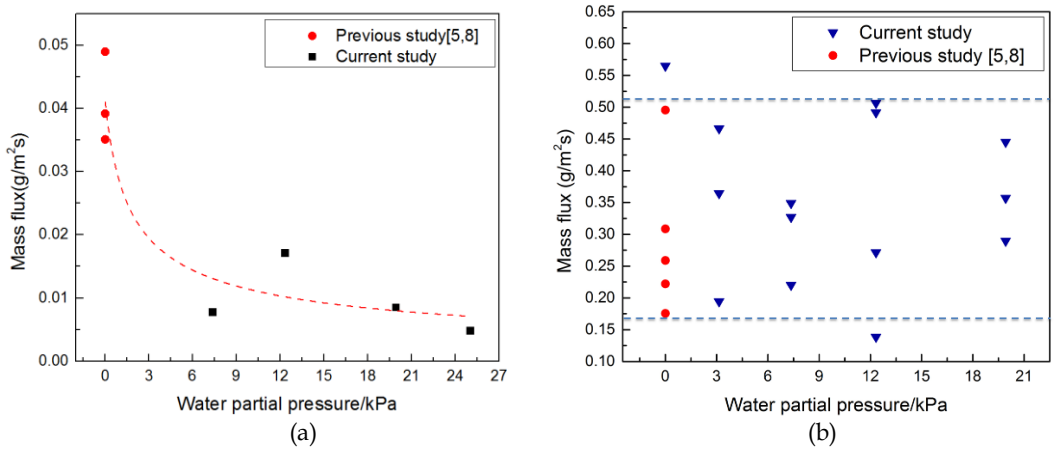

Fig.2 Measured mass flux of SiMn as a function of water pressure at, (a) 1450°C and (b) 1600°C

The mass flux at 1450°C in Figure 2(a), shows a significant decrease when the wet air is introduced in the experiments. As MnO is the main fume-forming gas at this temperature[5], the decreasing mass flux of fume behaves as expected, which is similar to the oxidation process of FeMn alloy under the same wet air conditions[4]. There were visible gas blisters formed on top of the metal after the experiment, and the size of the blisters tended to increase with the increasing water pressures. The mass flux at 1600°C is shown in Figure 2(b). There are significant variations between the repeated experiments under the same water contents of the gas. For these wet air experiments, there were visible oxide/slag areas formed on top of the metal surface after experiments. The passivation of the metal surface, forming oxide slag in addition to the fume, resulting in a non-static fuming surface, may explain the large deviations between experimental repeats at identical gas composition[10-12]. While results show variation, the trend indicate that the introduction of water to the system does not significantly change the total mass flux from the melt.

Scanning electron microscopy (SEM)

Fume samples from the 1600°C dry and wet air experiments were characterized in a scanning electron microscope (SEM). The equipment used was a Zeiss Supra 55 PV field emission microscope. The samples were held on a carbon tape, and the images were recorded at an acceleration voltage of 2-10 kV, with magnifications 2-50 k. Typical fume morphology and the fume compositions obtained from SEM and SEM-EDS are shown in Figure 3 and Table II.

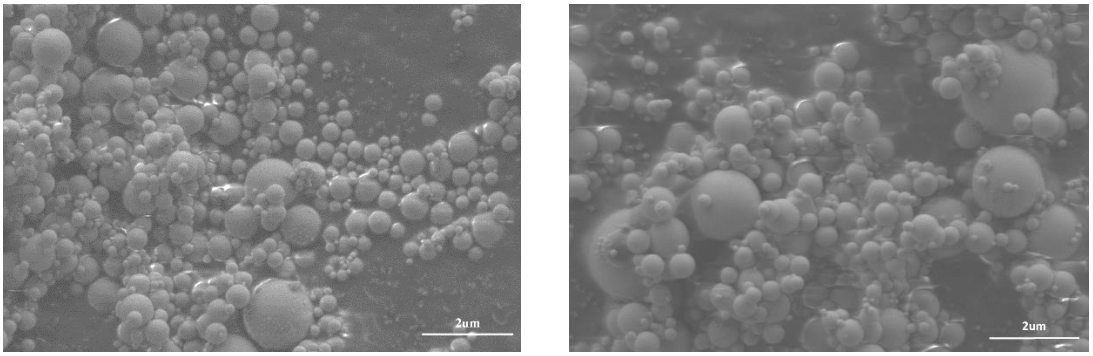

(a) (b)

Fig. 3 Typical fume morphology at 1600°C with, (a) dry air conditions, (b) wet air conditions

Table II. Compositions of fume particles at 1600°C wet air conditions, detected by SEM-EDS

SiMn fume compositions	1600°C
Major elements	Si, Mn, O
Minor/trace elements	Na, Mg, K, S, Al, Ca

Most of the fume particles generated under wet air conditions, seen in Figure 3(b), show spherical shapes with various sizes, which is the same as dry air experiments, seen in Figure 3(a), in our previous studies [5]. Visual and microscopic observation indicate that more agglomerates are formed in wet air conditions than dry air conditions, and further study into this dependency is under way. The wet air fume compositions , which were detected by EDS point analysis in the SEM, are listed in Table II. The major elements are Si, Mn and O, while the minor/trace elements detected are Na, Mg, K, S, Al and Ca. This is in accordance with previous (dry air) results[5].

X-ray diffraction (XRD)

All the fumes collected from different exhaust system positions for the 1600°C experiments for dry air and 4 different water pressures, were analysed by XRD (Bruker D8 Advance DaVinci X-ray Diffractometer). Different phases found by XRD are shown in Figure 4.

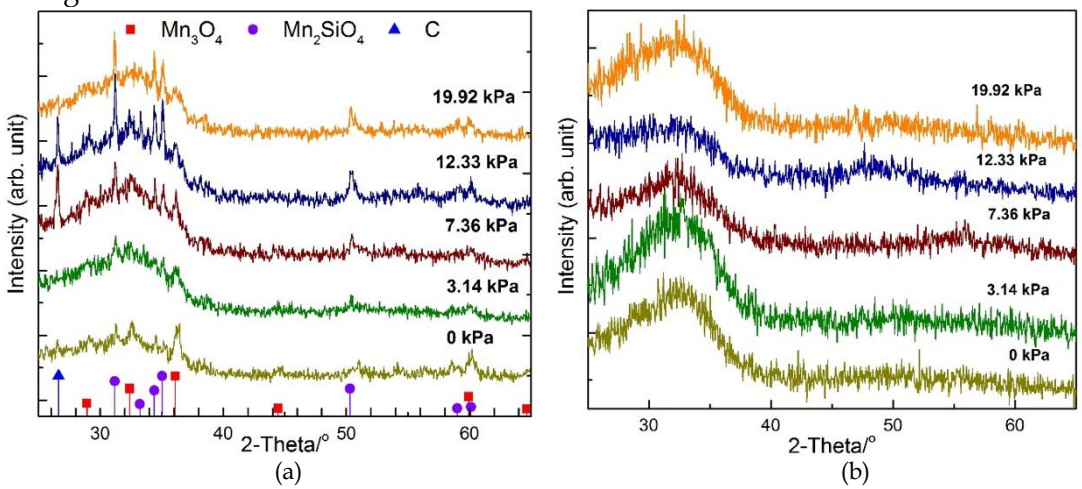

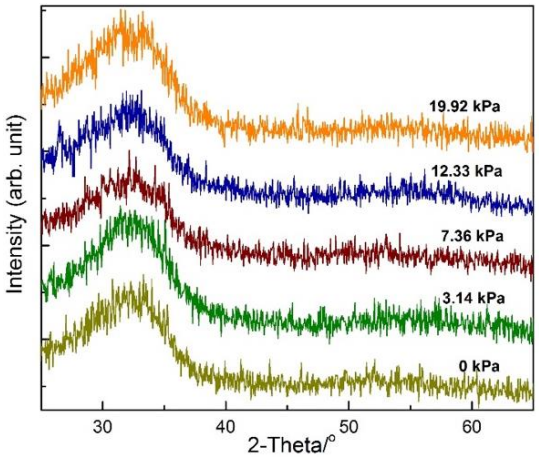

(c)

Fig.4 XRD diffraction patterns of the fume in; (a) transition tube fume, (b) cooler fume, (c) filter fume

As shown in Figure 4, crystalline phases are only detected in the transition tube fume, while amorphous phases dominate in both the cooler and filter fumes. The fumes formed under different water pressures show the same phases as the dry air experiments. The small amount of crystalline Mn_3O_4 formed in the transition tube fume can be explained by the deposition temperature in the transition tube about 600°C, where MnO may get further oxidize.

THERMODYNAMIC MODELLING RESULTS

In order to explain the experimental results from a thermodynamic perspective, equilibrium simulations of the experiments were performed using FactSage 7.1 thermochemical software[13]. The thermodynamic description of the SiMn melt was taken from the FTlite database, and those of oxides were taken from the FToxide database. Thermodynamic properties of pure substances including gas species were adopted from FactPS database. Thermodynamic modelling was carried out under the following assumptions:

- The melt was carbon saturated (2wt% C ~dissolves in the metal), as a graphite crucible was used during the experiments.
- The melt temperature and gas temperature of 1600°C was used for modelling.
- Dividing the melt bulk into a definite number of reaction volumes (e.g. 10 reaction volumes), assume 10% of the melt adiabatically reacted with the gas jet, simulating a time step (starting from the gas jet reacts with the melt, until the reaction reaches equilibrium) in the entire process. The modelling results in Figures 5 and 6 represent only a time step.
- Scheil accumulated cooling was applied to cool down the fume.
- The temperature across the melt-bulk air interface (boundary layer) was assumed to be constant.
- The oxygen partial pressure across the gas boundary layer was set to vary from 10^{-15} atm (P_{O2} in equilibrium with the C-saturated SiMn melt) at the metal interface to an oxygen partial pressure of 0.21 atm, i.e. the bulk air partial pressure.

Modelled oxidation reactions in the metal/gas boundary layer

The modelled reaction products from the oxidation reaction between the melt and the gas jet (synthetic air with water vapour) are shown in Figure 5. The figures a) and b) may be read as illustrating the reaction product composition throughout the gas boundary layer above the metal from the metal interface at the left of the figure to the bulk gas interface on the far right of the x-axis. Since the reaction between the melt and the gas jet

is adiabatic, the interface temperature locally increases above the process temperature of 1600°C. Each line in Figure 5 was calculated at a constant temperature enforced by the melt and gas jet adiabatic reaction. As shown in Figure 5a, the oxidation reaction products consist of two phases, an oxide liquid solution (labelled as liquid phase, and expanded in Figure 5b) and the gas phase. They are both very sensitive to the oxygen partial pressure. With increasing the oxygen partial pressure across the boundary layer from the value in equilibration with the melt (10^{-15} atm) to the bulk air almost 0.21 atm, somewhat more (small variations) gaseous phase and less liquid phase form with increasing water vapour pressure. With the oxygen partial pressure smaller than 10^{-12} atm, there is almost no liquid phase products generated. However, the gas phase products dominate in the products, the mass of the liquid phase product is one order of magnitude smaller than that of the gas phase product. The main conclusion is that there is no significant difference in the amount of oxidation reaction products in both gas phase and liquid phase with different moisture contents at 1600°C, which is consistant with the experimental results.

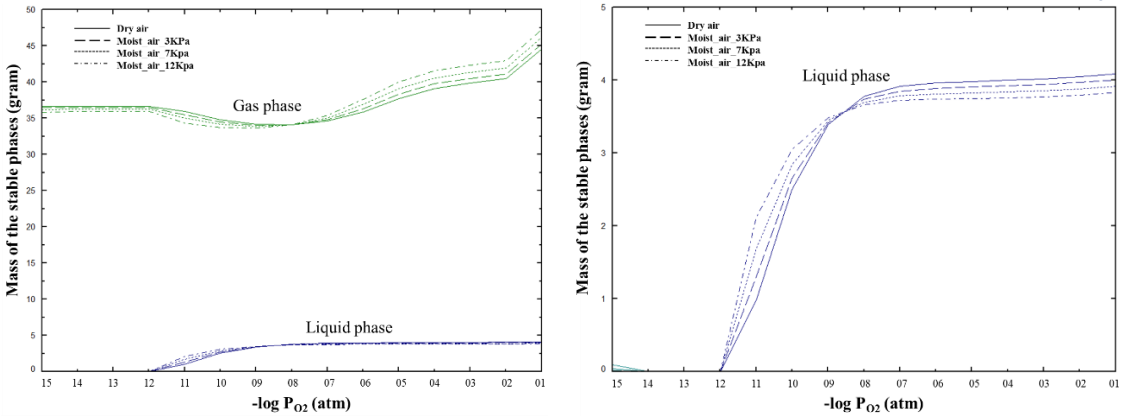

Fig.5 Calculated reaction products under different oxygen partial pressures (each line was calculated at a constant temperature enforced by the melt-gas jet adiabatic reaction), (a) gas phase and liquid phase products , and (b) enlarged liquid phase product.

Modelled fume compositions

As there are other gases consuming oxygen, e.g. the formation of CO(g), the oxygen partial pressure at the bulk air interface was assumed to be about 10^{-3} atm. Thus reaction products generated at oxygen partial pressure of 10^{-3} atm were cooled with Scheil cooling, and the modelled condensed phase - fume compositions - were obtained and shown in Figure 6. Part of the gas phase products exited the system as the off-gas, e.g. N_2(g), CO(g) and CO_2(g).

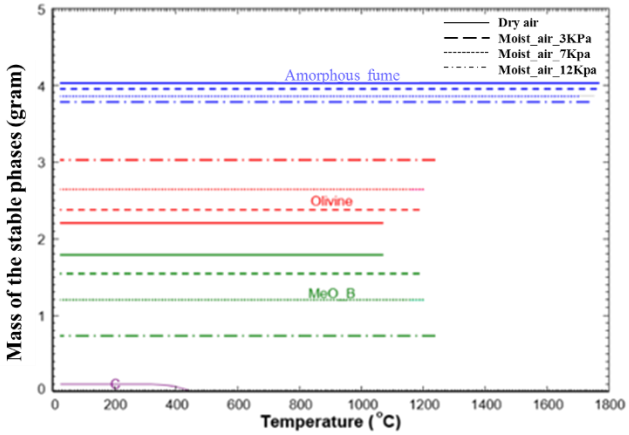

Fig.6 Calculated fume compositions by using scheil cooling

As illustrated in Figure 6, the modelled fume consists of an amorphous fume, olivine and MeO. The amorphous fume is from quenched oxide liquid phase products, Olivine and MeO are both quenched gas phase products. For dry air experiments, C also precipitates out of the fume below 450°C. The olivine phase is mainly composed of Mn_2SiO_4. The MeO phase is a solid solution of mostly MnO with less than 1.0 wt% Mn_2O_3 and below 0.10 wt% iron oxides. With increasing water pressures, the amount of amorphous fume and MeO phases in the fume decrease while that of olivine Mn_2SiO_4 increases. It also shows that there is almost no difference in the amount of fume generated with the increasing water contents, but the compositions of the fumes are different.

Correlation between modelled and experimental results

The modelled results confirms the experimental observations that there is no significant difference in the amount of fume generated with different moisture contents for SiMn at 1600C°. However, in the experimental system, the formation of slag on the liquid metal surface may have inhibited the fume formation.

The crystalline phases (Olivine and MeO) and amorphouse phase in the modelled fume are in almost equivalent (low) concentrations, while the main phase in the experimental fumes is amorphous, with only a small amount of Mn_3O_4 and Mn_2SiO_4 detected in the XRD results. The explanation could be that the Scheil cooling method used in the modelling and the real experimental cooling conditions are different.

There are observations of increased Mn_2SiO_4 generation and reduction in MnO generation with the increasing water pressure in the modelled results. The reduction of MnO behaves as expected. These observations will be further investigated in subsequent experimental and characterisation studies.

CONCLUSIONS

The effect of water vapour on the fume formation during the oxidation of an industrial SiMn alloy has been studied. It was found that:

- The mass flux of fume formed from the alloy held at 1450°C decreased under the wet air conditions, showing similar behaviour as FeMn alloys.
- The total mass flux of fume formed at 1600°C under various water pressures is similar to that of the dry air experiments. However, there are deviations between experimental repeats due to the formation of oxide slag on the metal surface.
- Typical fume morphologies and crystalline phases formed at 1600°C are the same as those with the dry air experiment, e.g, mainly amorphous phase, small amout of crystalline Mn_2SiO_4 and Mn_3O_4. Experimental and modelelled results are in agreement on the type of fume products formed. The deviations are likely caused by the different cooling conditions between model and real life.
- Factsage modelling results indicate that the fume formation is very sensitive to the oxygen partial pressure within the boundary layer. However, there is less MnO and more Mn_2SiO_4 in the modelled fume with increasing water vapour pressures. This finding will need to be confirmed by elemental fume analysis.

Further studies will be carried out with respect to the fume composition in terms of main elements (Si and Mn) and the particle size distributions under different water pressures.

ACKNOWLEDGEMENTS

Funding from the Norwegian Ferroalloys Research Association (FFF), Saint Gobain, Washington Mills and the Norwegian Research Council through the DeMaskUs project (contract 245216) is gratefully acknowledged. The authors would like to thank Kathrine Sellevoll for the assistance in carrying out the experimental work.

REFERENCES

1. *IMnI , H., IMnI LCA Summary Report View 2015.*
2. Sarel J. Gates, G.K., Steven C. Rencken, Neil M. Fagan, Peter Cowx, Luther Els,, *The use of fine water sprays to suppress fume emissions when casting refined ferromanganese.* The Clean Air Journal, 2015.
3. P. Cowx, R.N., M. Kadkhodabeigi, L. Els, I. Kero, *The use of fine water sprays to suppress fume emissions when casting refined ferromanganese*, in *Infacon XIV*. 1-4 June 2015: Kyiv, Ukraine.
4. Gates, S.J., et al., *The Influence of Water Vapour on the Fuming Rate in a Ferromanganese System*, in *Energy Materials 2017*, X. Liu, et al., Editors. 2017, Springer International Publishing: Cham. p. 73-83.
5. Ma, Y., I. Kero, and G. Tranell, *Fume Formation from Oxidation of Liquid SiMn Alloy.* Oxidation of Metals, 2017.
6. Næss, M.K., et al., *Parameters Affecting the Rate and Product of Liquid Silicon Oxidation.* Oxidation of Metals, 2014. **82**(5-6): p. 395-413.
7. Kero, I. and G. Tranell, *Active oxidation and fume formation from liquid SiMn*, in *TMS Annual Meeting*. 2016: Nashville, USA: John Wiley & Sons, Inc., Hoboken, New Jersey. p. 77-84.
8. Ma, Y., et al., *Trace Elements Behavior During the Oxidation of Liquid SiMn Alloy*, in *8th International Symposium on High-Temperature Metallurgical Processing*, J.-Y. Hwang, et al., Editors. 2017, Springer International Publishing: Cham. p. 215-224.
9. Genskow, L.R., et al., *Psychrometry, Evaporative Cooling and Solids Drying*, in *Perry's Chemical Engineers' Handbook*, W. Green, Editor. 2008, McGra-Hill Companies Inc.: United States of America. p. 3-6.
10. Safarian, J., et al., *Boron Removal from Silicon by Humidified Gases.* Metallurgical and Materials Transactions E, 2014. **1**(1): p. 41-47.
11. Sortland, Ø.S., *Boron removal from silicon by steam and hydrogen*. 2015, Norwegian university of science and technology.
12. Altenberend, J., *Kinetics of the plasma refining process of silicon for solar cells: experimental study with spectroscopy*. 2012, UNIVERSITÉ DE GRENOBLE.
13. Factsage, *Factsage 7.1*. 2017.

Yan Ma
PhD candidate, NTNU
With a master degree of industrial ecology and metallurgical engineering from University of Science and Technology Beijing. Research areas within emissions from metallurgical industry and coal power plant.

Presenting author

Gabriella Tranell
Professor,NTNU
Professor at the Department of Materials Science and Engineering, Extractive Metallurgy Group, NTNU.
Research Areas: Production of Ferroalloys, Production and Refining of Silicon, Solar Cell Materials, Environmental issues and emissions from the metallurgical industry, Recycling of metals.